applied sciences

MDPI

Article

A New Technology for Smooth Blasting without Detonating Cord for Rock Tunnel Excavation

Chunde Ma [1,2], Weibin Xie [1], Zelin Liu [3,*], Qiyue Li [1], Jiaqing Xu [1] and Guanshuang Tan [1]

1 School of Resources and Safety Engineering, Central South University, Changsha 410083, China; cdma@csu.edu.cn (C.M.); weibin@csu.edu.cn (W.X.); qyli@csu.edu.cn (Q.L.); xu1001@csu.edu.cn (J.X.); tanguanshuang@csu.edu.cn (G.T.)
2 Advanced Research Center, Central South University, Changsha 410083, China
3 School of Civil Engineering, Central South University, Changsha 410075, China
* Correspondence: zelinl@csu.edu.cn

Received: 6 September 2020; Accepted: 25 September 2020; Published: 27 September 2020

check for updates

Featured Application: For the first time, we successfully measured the critical distance of rock emulsion explosive under the constraint of blasthole, which was about 1.0~1.1 m. Based on the critical distance, a smooth blasting technology without detonating cord was designed, which can achieve the purpose of simplifying the working procedure, saving costs and improving efficiency.

Abstract: In this paper, the aim is to achieve safe, rapid excavation of an extra-long, large-cross-section highway tunnel in Eastern Tianshan, as well as to reduce production costs, simplify production processes, reduce cycle time, and improve production efficiency. In this study, we explored a new technology for smooth blasting without a detonating cord. A series of sympathetic detonation experiments were conducted in the tunnel face to determine critical distances. The critical distance for No. 2 rock emulsion explosive under blasthole constraints was successfully measured to be approximately 1.0–1.1 m. Based on the critical distance, a new charging structure was designed for tunnel excavation. To assess the influence of the new charging structure on blasting performance, its economic benefits, and its feasibility, full-section tests were performed in the East Tianshan Tunnel. The application of the new charging structure produced good smooth blasting results. It not only simplified the charging process and produced smooth blasting without detonating cord in peripheral holes, but also guaranteed normal excavation, an appropriate tunnel profile, and reasonable overbreak and underbreak volumes. This had remarkable economic benefits and possesses better promotional value.

Keywords: rock tunnel excavation; smooth blasting; sympathetic detonation; critical distance; new charging structure; no detonating cord

1. Introduction

In modern tunneling development, smooth blasting technology is widely used for tunnel excavation in order to control tunnel profiles, decrease overbreak and underbreak volumes, and reduce vibration damage to surrounding rock caused by blasting in peripheral holes [1–3]. To achieve a good smooth blasting effect, air-decked charge technology has become a popular method [4–6]. In addition, smooth blasting parameters have been continuously optimized for tunnel construction [7–9].

For smooth blasting, explosives were generally in the form of air-decked decoupled charges. However, explosives may self-extinguish or refuse to blast in a blasthole because of the channel effect or excessively long gap distances between explosives [10]. The full-length detonating cord detonation propagation method is usually used in blastholes, as shown in Figure 1. In tunnel excavation projects with large cross-sections, the number and depths of peripheral holes are large and the unit price of detonating cord is expensive compared to those of other blasting materials such as explosives and detonators. Because of this, the consumption of detonating cord accounts for a large proportion of the smooth blasting cost in tunnel construction. In addition, the laying of detonating cord wastes a lot of time and increases the labor intensity of the project. Therefore, the cancellation of the detonating cord is of great significance to speed up the construction progress and reduce economic losses. Furthermore, tunnel excavation has a large impact on the surrounding environment. Blasting vibrations and high-stress release from the excavation process can cause safety hazards. It is critical to transform the traditional production strategy into a safe, clean, efficient production system [11–13].

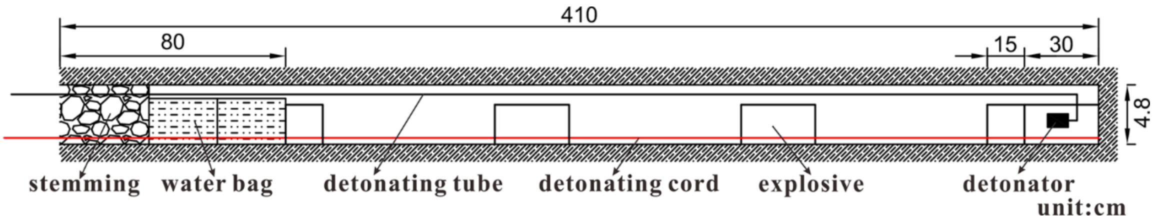

Figure 1. Schematic diagram of a traditional charging structure.

According to the characteristics of sympathetic detonation, in practice, if the critical distance between two explosives is large enough, it is possible for explosives in blastholes to be completely detonated without detonating cord. This can produce smooth blasting without use of detonating cord. In sympathetic detonation, the detonation of an explosive (donor charge) triggers another nearby explosive (acceptor charge). The critical distance is the maximum distance between donor and acceptor charges that allows sympathetic detonation to occur [14,15]. Researchers have conducted significant studies on sympathetic detonation in recent decades. Victor [15] introduced a simple but detailed calculation method that could predict sympathetic detonation of cylindrical explosives. The calculated results compared well with the experimental results. Ko et al. [14] conducted a water-container gap test to obtain the critical distance for a shaped charge in underwater sympathetic detonation and performed a numerical interpretation of the critical distance. Kubota et al. [16] carried out a numerical simulation of a gap test on sympathetic detonation. The results revealed that there is a logarithmic-scale linear relationship between the critical gap length and the explosive diameter. DeFisher et al. [17] carried out a numerical simulation of sympathetic detonation of an explosive with a shell and analyzed the influences of various spacing and buffer materials on sympathetic detonation. Chen et al. [18] conducted laboratory experiments and numerical simulation studies on cylindrical GHL (RDX/Al/binder) explosives with shells to determine critical distances and analyze shell damage mechanisms. Ishikawa et al. [19] conducted a series of gap tests with various gap materials and explosive quantities to determine the critical gap lengths for various explosive quantities and describe the relationship between the quantity of explosive and shock sensitivity. Chen et al. [20] determined the critical distances for emulsion explosives under various constraint conditions and the attenuation law for the detonation velocities of acceptor charges at various interval charge distances. The results revealed that external constraints have substantial influence on the critical distances of emulsified explosives. Better constraint conditions can more substantially increase the critical distance. Katsabanis [21] carried out sympathetic detonation experiments in blastholes and found that the pressure in the blasthole stemming decreased but the pressure at the acceptor charge increased. He also pointed out that sympathetic detonation is caused by the deflagration to detonation. Zhang [22] established an empirical formula for the gap distance between explosive cartridges in the blasthole. This laid the foundation for calculation of the critical distance in a blasthole.

Through the above analysis, it can be found that those factors like explosive diameter, spacing and buffer materials, explosive quantities, and constraint conditions are all related to sympathetic detonation critical distance. Hence, it is vital to investigate the measurement of critical distances for explosives under the constraint of a blasthole. However, there is still a lack of research that includes sympathetic detonation tests under the constraint of a blasthole.

In this paper, the tunnel project of the East Tianshan Tunnel in the Xinjiang Uygur Autonomous Region of China was used as an example. We seek to optimize and adjust the current charging structure to achieve smooth blasting without detonation cord in peripheral holes. This helps to accelerate construction progress and reduce the cost of smooth blasting. To obtain the critical distance for sympathetic detonation under the constraint of blasthole, preliminary gap tests are performed using No. 2 rock emulsion explosive. The traditional smooth blasting charge structure used in the East Tianshan tunnel is optimized and adjusted based on the critical distance. A series of full-section tests are conducted and the results are analyzed to assess the feasibility of using the new charging structure in the East Tianshan Tunnel.

2. Sympathetic Detonation Experiments

2.1. Background

The experiments were performed in the East Tianshan Tunnel, which is a control project for the G575 line from Balikun to Hami in the Xinjiang Uygur Autonomous Region, China. It has a total length of 11.9 km and a maximum depth of about 1200 m. The tunnel is located in a high-altitude, cold, mountainous area and crosses the Tianshan Mountains. The surrounding rock in the tunnel is generally graded III–IV, and the surrounding rock in the entrance, exit section, and fracture zone is graded IV–V, the grading type for surrounding rock of highway tunnel as shown in Table 1. The topography, geology, hydrology, and meteorological conditions are quite complex. High in-situ stress phenomena form easily and there is substantial risk of encountering serious geological hazards such as rock burst during construction.

Table 1. Grading for surrounding rock of highway tunnel.

Grading Type	Features of Surrounding Rock	Basic Quality Index of Surrounding Rock (BQ)
I	Hard rock, complete rock mass, huge monolithic or huge thick layered structure.	>550
II	Hard rock, relatively complete rock mass, massive or thick layered structure. Relatively hard rock, complete rock mass, block overall structure.	550~451
III	Hard rock, relatively broken rock mass, massive fragment mosaic structure. Relatively hard rock or softer rock layer, rock mass is relatively complete, massive or medium-thick layer structure.	450~351
IV	Hard rock, broken rock mass, fragmented structure. Relatively Harder rock, the rock mass is between relatively broken and broken, with inlaid fragmented structure. Soft rock or soft and hard rock interbedded, and mainly soft rock, the rock mass is relatively complete to relatively broken, with a medium-thin layered structure.	350~251
V	Soft rock, rock mass is relatively broken to broken. Relatively soft rock, broken rock mass. Extremely broken rock mass. Broken, cracked and loose structure.	≤250

Note: BQ = 100 + 3Rc + 250Kv, where Rc is Uniaxial saturated compressive strength of rock, Kv is Rock mass integrity factor.

The surrounding rock of the test section is mainly breeze tuffaceous sandstone, which is blue-gray and gray-green, with gray-green diabase and quartz diorite veins distributed locally, and the surrounding rock is grade IV. The rock mass is complete, the rock mass is dense and hard, and the surrounding rock has good self-stability. In the test rounds, the surrounding rock conditions did not change significantly, which ensuring the reliability of the test results.

2.2. Experimental Scheme

The most effective way to obtain critical distance is gap test [23]. The gap test conducted in the peripheral holes required a donor charge, an acceptor charge, and a blasthole. Since these were gap distance tests, there was no need to place a spacer between the donor and acceptor charges. So that the experimental area would not be covered by accumulated blasting slag and for convenient post-experiment observation, the test blastholes were selected from the peripheral holes at the upper left and upper right of the tunnel face. The test blastholes for sympathetic detonation tests were continuous, without mutual interference and in the same group of blasting networks (Figure 2). The blasthole diameter was 4.8 cm, the average depth was 410 cm, and the peripheral hole spacing was 50 cm. The test blastholes used the charging structure shown in Figure 3 and the remaining blastholes were charged using the traditional charging structure. For the sympathetic detonation tests, No. 2 rock emulsified explosive was used in both the donor and acceptor charges, the cartridge length was 300 mm, the cartridge diameter was 32 mm, and the cartridge density was 0.95–1.30 g/cm^3. All explosives were charged into blastholes in the rock and detonated in a prearranged sequence. Corresponding marks were placed on the rock near the test blastholes in order to accurately identify their positions after blasting. In order to prevent tunnel construction affecting the sympathetic detonation experimental results, it was necessary to observe sympathetic detonation and record the test phenomena immediately after blasting was completed.

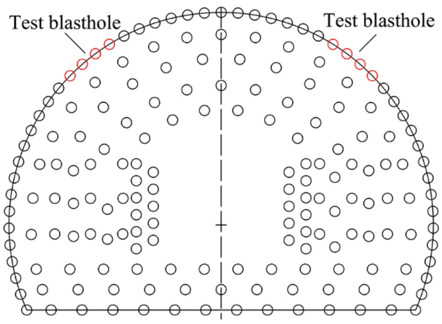

Figure 2. A diagram that shows test blasthole locations.

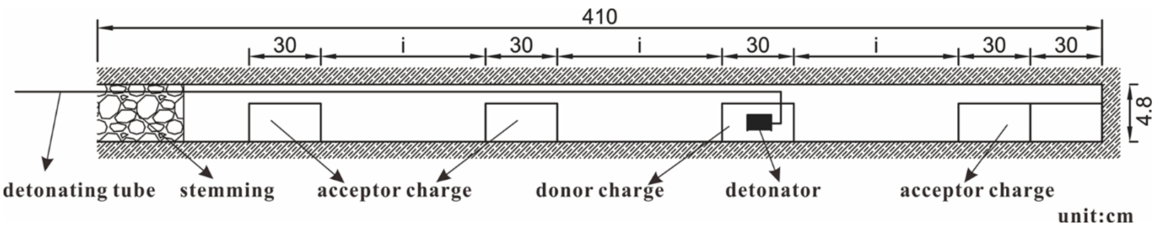

Figure 3. Schematic diagram of the charging structure used for gap distance testing.

In order to measure the critical distances for explosives under the constraint of a blasthole without affecting normal tunneling construction, it was necessary to ensure that the explosives could blast steadily. According to Chen et al. [20], the critical distance is greater under a constraint than in open air. The critical distances of No. 2 rock emulsion explosive under the constraints of PVC pipe, φ40 mm low-carbon iron pipe, stainless steel pipe, and φ50 mm low-carbon iron pipe were 10–20 cm, 70–80 cm, 60–70 cm, and 30–40 cm, respectively. Hence, we started our gap distance tests from 70 cm. If sympathetic detonation of the acceptor charge occurred, we increased the gap distance and continued the test.

2.3. Results and Discussion

Table 2 records the results of various blasthole gap distance tests. The experiments were performed six times. Because of the blasting and excavation processes, the tests performed at 70 cm, 80 cm, and 100 cm were only carried out in two blastholes. This did not affect the reliability of the test results.

Table 2. Test results for sympathetic detonation in blastholes.

Gap Distance (cm)	Number of Blastholes	Test Results
70	2	Half-hole traces were clear, the blasting effect was good, and all explosives blasted.
80	2	Half-hole traces were clear, the blasting effect was good, and all explosives blasted.
90	4	Half-hole traces were clear, the blasting effect was good, and all explosives blasted.
100	2	Half-hole traces were clear, the blasting effect was good, and all explosives blasted.
110	4	The blasting effect at the bottom of the blasthole was good but about 20 cm of surrounding rock at the orifice of some blasthole didn't drop fully.
120	4	The blasting effect at the bottom of the blasthole was good but about 50 cm of surrounding rock at the orifice of some blasthole didn't drop fully.

Figure 4 show the traces of blastholes at the scene after the first, fourth, fifth and sixth sympathetic detonation.

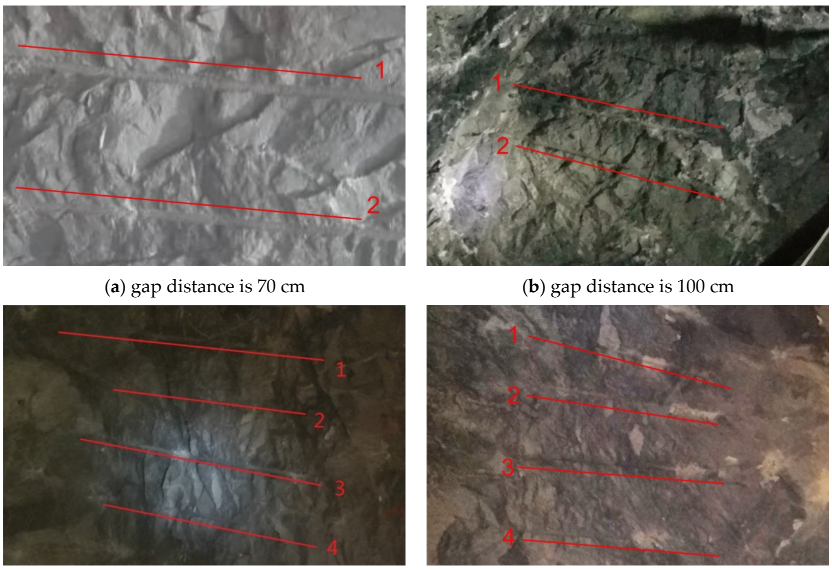

(**a**) gap distance is 70 cm (**b**) gap distance is 100 cm

(**c**) gap distance is 110 cm (**d**) gap distance is 120 cm

Figure 4. The traces of blastholes of various gap distances on sympathetic detonation. (**a**) gap distance is 70 cm, (**b**) gap distance is 100 cm, (**c**) gap distance is 110 cm, (**d**) gap distance is 120 cm.

According to Table 2 and Figure 4, when the gap distance is 0.7–1.0 m, the rocks around the testing blasthole are blasted and dropped and there are clear marks from the blasthole half-holes. There are no traces of residual cartridges on the blastholes and the sympathetic detonation effect meets experimental requirements overall. However, when the gap distance increases to 1.1 m or 1.2 m, the bottom of the blasthole exhibits good blasting effects and there are clear blasthole half-hole marks, but some of the rock surrounding the orifices of some blastholes does not blast fully. This phenomenon is explained as follows: (1) The explosives at the bottom of the blasthole always exhibit sympathetic detonation but one cannot determine whether the blasthole gap distance is 1.1 m or 1.2 m. Because the bottom of the blasthole is an infinite rock mass, it can reflect and strengthen the shock wave. This effect supports sympathetic detonation. (2) Explosives at the blasthole orifices may undergo sympathetic detonation, but 1.1 m and 1.2 m are close to the limit at which this might not occur. Because of this, acceptor charge detonation propagates unsteadily. This results in poor blasting results at the orifice. (3) Gap distances of 1.1 m and 1.2 m can lead to sympathetic detonation of the acceptor charge. However, due to stemming quality limitations, the explosives near the orifice may be pushed outside of the blasthole by high-temperature, high-pressure gas during blasting. This leads to an uneven explosive distribution along the blasthole and results in poor blasting effects at the blasthole orifice. Therefore, the critical distances for No. 2 rock emulsion explosive are 1.0 m at the blasthole orifice and 1.1 m at the bottom of the blasthole.

Under unconstrained conditions (in open air), the detonation wave and products generated after the explosive blast spread directly in all directions and do not converge, as shown in Figure 5a. For sympathetic detonation of an acceptor charge to occur, the distance between the donor and acceptor charges must be quite small. The existing research [20,22] states that this distance is only approximately 5 cm. Nevertheless, under blasthole constraints, the detonation wave and products do not act directly on the hole wall, but rather fill the hole before acting on the hole wall. Under the blasthole constraint, the lateral dispersions of the detonation wave and products are reduced. Since many detonation waves propagate along the axial direction of the blasthole, the critical distance in the blasthole increases substantially, as shown in Figure 5b. The gap test results indicate that the critical distance under the blasthole constraint is approximately 100–110 cm, which is about 20 times that noted under unconstrained conditions. Thus, the influence of a constraint on the blasting distance is huge. The empirical formula for the critical distance for explosive cartridges in a blasthole is [22]:

$$\mathrm{M} = \frac{K}{2}\left[\frac{(2m+d)^2(2m+L)}{D^2} - L\right] \tag{1}$$

where M is the critical distance for explosive cartridges in the blasthole, m is the critical distance for the standard experiment in open air, which is indicated on the product performance sheet, d is the explosive cartridge diameter, D is the blasthole diameter, L is the explosive cartridge length, and K is the attenuation coefficient, which is 0.8–0.9.

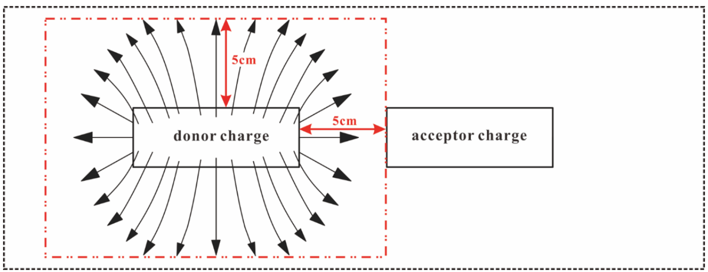

(a) under unconstrained conditions

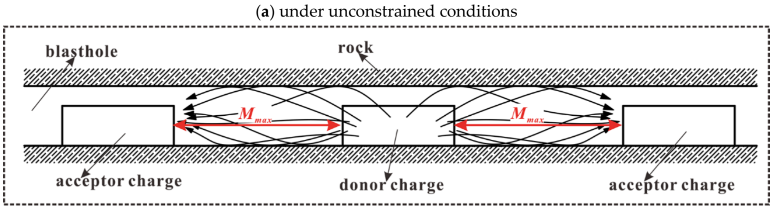

(b) under blasthole constraints

Figure 5. Propagation of detonation waves and products under various constraints. (**a**) under unconstrained conditions, (**b**) under blasthole constraints.

According to Equation (1), the critical distance in the blasthole is 109 cm. This fits with the field experiment results and confirms their accuracy to some extent.

3. Application of the New Charging Structure

3.1. Charging Structure Optimization Analysis

Using the sympathetic detonation experiments that we conducted under blasthole constraints, the traditional charging structure was optimized and upgraded based on the explosive critical distances. The new charging structure shown in Figure 6 was thus designed. The new charging structure is divided into three parts. The bottom of the blasthole contains a fortified charge. Two rolls of explosives are charged at this position. Such a quantity is conducive to overcoming the resistance line and clamping effects at the bottom of the blasthole. The middle of the blasthole contains a normal charge. Because the detonating cord contains black sorkin, if charged according to the traditional charging structure, it is equivalent to 50 g black sorkin in each peripheral hole. Since the power of black sorkin is greater than that of the emulsion explosive and the new charging structure removes the detonating cord, it is necessary to charge at least 50 g of extra emulsion explosive per hole when the new charge structure used. To facilitate charging, 1.5 rolls of explosives are charged at this position as the donor charge. This increases the detonation energy and facilitates sympathetic detonation. The blasthole orifice is decreasing charge part, where contains only 1 roll of explosive. In the new charging structure, each blasthole requires 4.5 rolls of explosives. The detonator uses reverse detonation, which is good at fragmenting rock mass at the plugging surface [24]. Meanwhile, it is important to ensure the quality of stemming at the blasthole orifice to ensure that sympathetic detonation of the explosive occurred at decreasing charge part. Moreover, it is important to ensure that the orifice is 65 cm away from the first roll of explosive during charging.

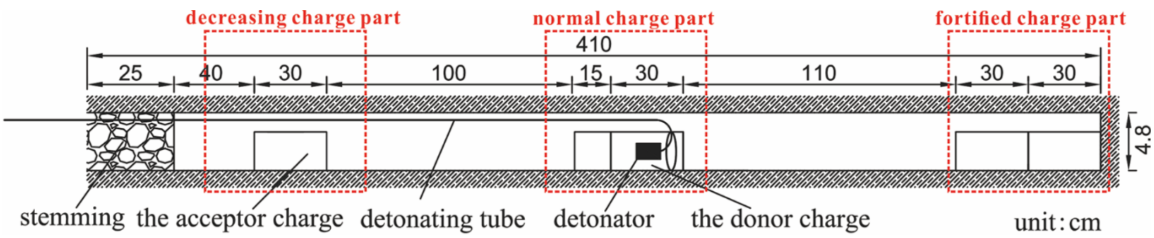

Figure 6. The new charging structure designed using the critical distance.

However, the blasthole length is likely to vary from 4.1 m in practice. From the gap distance tests and sympathetic detonation characteristics, one can see that when the distance between explosives is smaller than the critical distance, the acceptor charge can always be detonated by the donor charge. When the blasthole length is shorter than 4.1 m, the distance between explosives is decreased appropriately during charging. This aids sympathetic detonation. However, the insufficient blasthole length also causes reduction in cyclical footage, resulting in underbreak. When the blasthole length exceeds 4.1 m, we must guarantee that the distances between explosives are accurate, as shown in Figure 5. The following improvements may be made: (1) we can add a roll of explosive to the bottom of the blasthole; (2) the explosives can be placed 4.1 m away from the orifice instead of directly at the bottom of the blasthole; or (3) the quantity of explosives at the orifice can be increased to 1.5 rolls. Statistically, there are few blastholes with lengths greater than 4.1 m, so this situation does not have a large influence on application of this process.

3.2. Mechanism of the New Charge Structure

Figure 6 shows that application of the critical distance strategy only changes the distribution of explosives in the air-decked charging structure. The rock-breaking mechanism of the new critical distance-based charging structure is the same as that of the air-decked charging structure. The new charging structure is more advantageous than the air-decked charging structure because it removes the need for detonating cord and simplifies the charging process. Air-decked technology has been used for many years [25–27]. Existing research shows that the shock wave generated after an explosive blast acts on the rock surrounding the blasthole, as well as on the rock that it passes by during propagation to the air deck. This produces extensive microfractures on the surrounding rock surface. When the shock waves generated by the explosives at both ends of the air deck collide in the air column, they reflect, rebound, and move towards the bottom of blasthole and the direction of the stemming. This creates a secondary destructive effect on the rock that the shock waves pass by. Expansion and crushing act on the micro-cracks to crush the rock. Generally, the blast energy is redistributed after the air-decked charge is blasted. The explosive energy is first transferred to the air and then transferred to the rock by the air. The air column is used to reduce the initial pressure from the blasting products and increase the duration of interaction between the detonation wave front and the surrounding rock. The increased blasting time increases the rock fragmentation time and the rock is fully destroyed [28,29].

Air-decked techniques for rock fragmentation have achieved great success. Several researchers [26,27] have reported that use of air decking can improve the effective utilization of explosive energy and rock fragmentation uniformity, while reducing explosive consumption by 10–30% and decreasing blasting costs. Fourney et al. [30] observed the development of a fracture network in thick Plexiglass under the influence of an air-decked explosive, as showed in Figure 7. The shock wave reflected back-and-forth in the air column and the duration of the shock wave effect on the Plexiglass increased by a factor of 2–5. The above analysis indicates that the new charging structure is also suitable for rock-breaking. Furthermore, the distance between explosives in the new charge structure is more standardized, so the problem of detonation failure will be significantly improved.

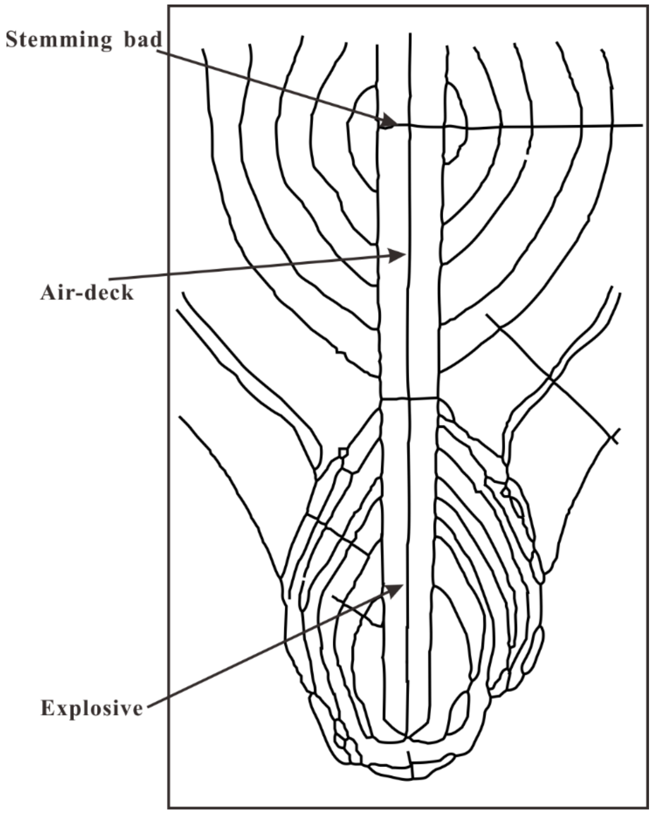

Figure 7. Fracture network development in thick Plexiglass [30].

3.3. Results and Discussion

To verify the availability of the new charging structure, three full-section tests were performed in the excavation face. The three tests used 34, 28, and 33 peripheral holes, respectively. The test blastholes were charged using the new charging structure mentioned above and paint was marked on the rock surrounding the corresponding test blastholes. The blasting effect was confirmed and the blasting traces were observed after blasting was completed.

After blasting, the test blastholes were identified using the marks. The three experiments show that the new charging structure meets smooth blasting requirements. There are visible half-hole traces on the tunnel wall, the explosive exhibits a good detonation propagation effect, and misfire does not occur. The rock surrounding the blastholes drops out and the outline contour forming effect is good. Thus, there is no need to refire. Figure 8 shows the smooth blasting results of the left, right side walls, and the arch crown of the tunnel cross-section after the first test. Since there are obvious half-hole traces and there is no explosive residue, sympathetic detonation of explosives occurs in the new charging structure.

(**a**) the left side wall (**b**) the arch crown (**c**) the right side wall

Figure 8. Smooth blasting results from the first test. (**a**) blasthole traces on the left side wall, (**b**) blasthole traces on the arch crown, (**c**) blasthole traces on the right side wall.

According to the statistics of recent cyclical footage in tunnel excavation, the cyclical footage of three tests was 3.5 m, 3.6 m, and 3.3 m, respectively. Figure 9 shows that the cyclical footage of the three full-section tests is at a normal level. Thus, the application of the new charging structure does not affect the normal tunnel excavation cyclical footage.

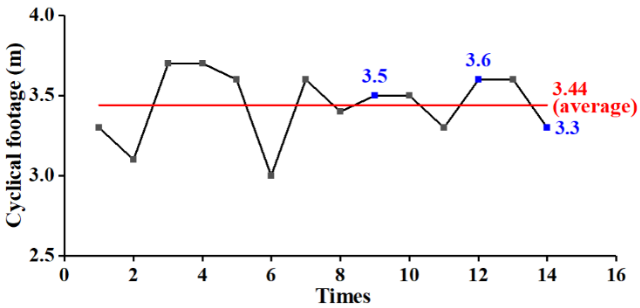

Figure 9. Tunnel excavation cyclical footage.

Figure 10 shows tunnel profile scanning photos after conventional blasting and full-section tests. Upon comparing tunnel profile scans, one can see that the tunnel profile control improves, the actual excavation profile is in good agreement with the theoretical one, the overbreak and underbreak volumes are normal, and blasting smoothness meets requirements. Figure 10 shows that reasonable amounts of overbreak and underbreak occur in some parts of the tunnel, regardless of whether the new charging structure is used. This can be dealt with in the planning section process and does not affect normal tunnel construction.

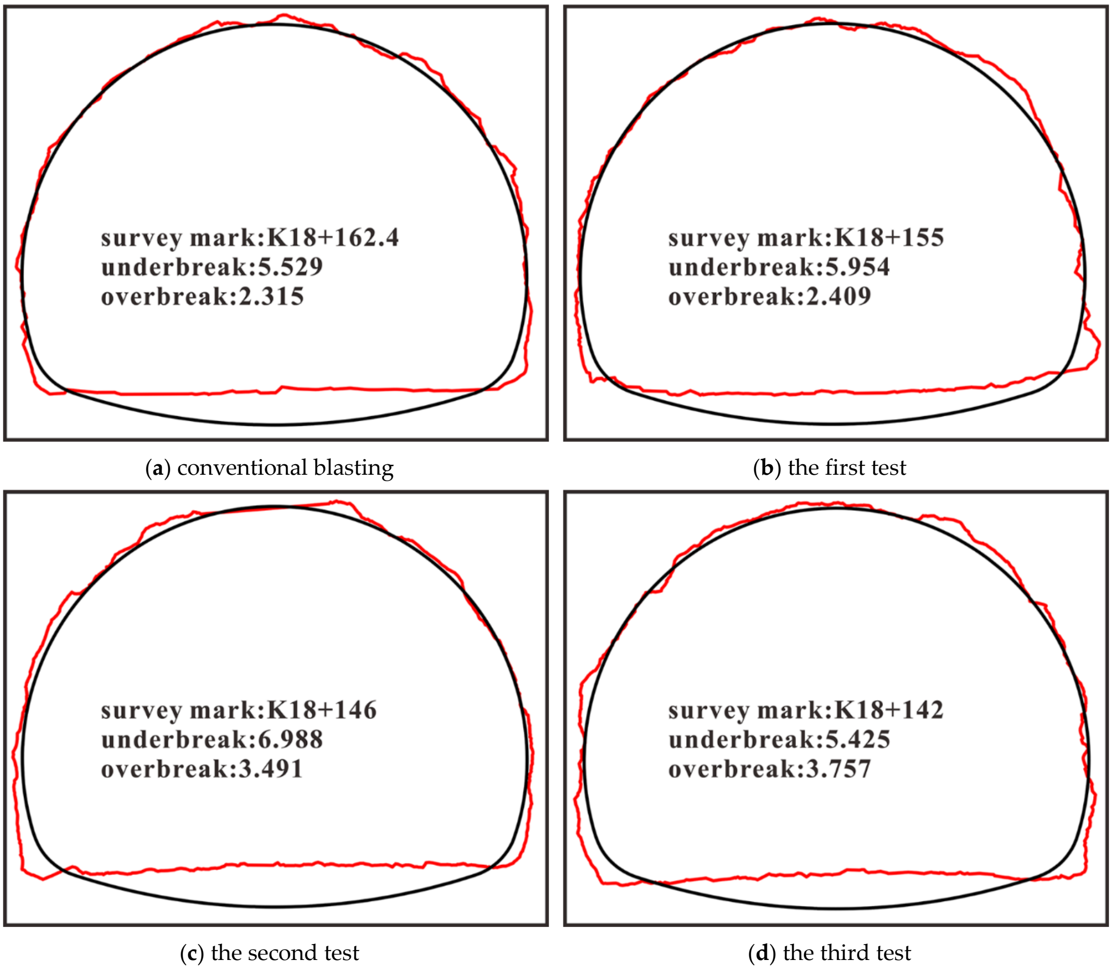

Figure 10. Scanning photos of tunnel profiles. (**a**) the actual and theoretical excavation profile of conventional blasting, (**b**) the actual and theoretical excavation profile of the first test, (**c**) the actual and theoretical excavation profile of the second test, (**d**) the actual and theoretical excavation profile of the third test.

Figure 10 were the tunnel profile scanning photos at the bottom of blastholes after blasting. Because the blastholes have a certain extrapolation angle, the overbreak/underbreak volumes at the at the bottom of the hole is the largest. The two-dimensional tunnel profile scanning at the bottom of blastholes can provide a reference for the overbreak/underbreak volumes of one excavation round to a certain extent. With the advancement of technology, compared with two-dimensional tunnel profile scanning, laser scanning or photogrammetry could better reflect overbreak/underbreak volumes of one excavation round. As demonstrated by Uotinen et al. [31], the use of laser scanning or photogrammetry could clearly record the rock surface geometry. Through photogrammetric reconstruction, a three-dimensional model is established and compared with the real tunnel environment, the rock excavation conditions on each cross-sectional profile can be extracted. Therefore, in the future, the tunnel profile would be scanned after each blasting round and the volume after blasting would be compared against the ideal, designed tunnel profile in three dimensions, rather than on the two-dimensional section.

Theoretically, the number of test blastholes should be 36, 31, and 41 in the three full-section blasting tests. However, we actually use 34, 28, and 33 test holes, respectively. Thus, the distance between blastholes is sometimes too large and underbreak occurs. Moreover, the average tunnel excavation cyclical footage is 3.44 m, but most blastholes are approximately 4.0 m in length and a few can be 4.5 m long. This reflects low blasthole and explosive energy utilization rates.

Every construction situation is different. The number of blastholes may be higher or lower and the blastholes may be long or short. These parameters affect the economics of construction. Therefore, this study calculates only the economic benefits of one excavation round under ideal conditions. The simulation is performed strictly according to the design drawings. Upon comparing the new and traditional charging structures, we see that each peripheral hole in the new charging structure requires 0.5 rolls of explosives more than the traditional structure. However, the traditional charging structure uses an additional 200 m of detonating cord. Under ideal conditions, the number of peripheral holes is 41. Table 3 compares the economic benefits of the new and traditional charging structures during an excavation round. Approximately 200 m of detonation cord is saved in one excavation round. The new charging structure reduces the blasting cost by 53.6%. Detonating cord accounts for a certain proportion of the cost of smooth blasting. Therefore, reducing the use of detonating cord and avoiding the transmission of detonating cord reduces production costs, simplifies processes; reduces cycle time; and improves production efficiency. This approach has broad blasting excavation application prospects and plays a decisive role in blasting technology improvement.

Table 3. Comparison of economic benefits.

Material	Unit Price	Traditional Charging Structure		New Charging Structure	
		Volume	Price/yuan	Volume	Price/yuan
Detonating cord	5.25 yuan/m	200 m	1050		
Explosive	4.5 yuan/roll	164 rolls	738	184.5 rolls	830.25
Total			1788 (100%)		830.25 (46.4%)

4. Conclusions

In this study, a set of sympathetic detonation experiments was performed to measure critical distances under blasthole constraints. Meanwhile, to evaluate the feasibility of the new charging structure, full-section tests were conducted in the peripheral holes of the tunnel face. Based on the study results, the main conclusions can be drawn as follows:

(1) The critical distance is an important explosive performance indicator. Based on gap tests under blasthole constraints, the critical distance for No. 2 emulsified explosives is about 1.0–1.1 m. The traditional charging structure was optimized using this critical distance to form a new charging structure that did not require detonating cord and simplified the charging process.

(2) Full-section test results show that the new charging structure can achieve smooth blasting without detonating cord in the peripheral holes. This can achieve the same smooth blasting effect as a traditional charging structure. The blasthole traces were clear, the overbreak and underbreak volumes were normal, and tunnel profile control was improved.

(3) The new charging structure provided good economic benefits. It could save 200 m of detonating cord and reduce the cost of smooth blasting by 53.6% per excavation round. The new charging structure removed the detonating cord, decreased the intensity of labor, and produced smooth blasting results. Thus, it has broad application prospects.

The successful application of the critical distance further improved smooth blasting technology. This technology is not very mature and perfect now, which is presently implemented only in the East Tianshan Tunnel. Specific experimental research should be done under other geological engineering conditions. However, the advantages of this technology show that it has significant application value.

Author Contributions: Conceptualization, C.M. and Q.L.; data curation, W.X. and Z.L.; funding acquisition, C.M. and Q.L.; methodology, W.X. and Z.L.; project administration, W.X.; supervision, C.M. and Q.L.; validation, Z.L. and J.X.; writing—original draft, W.X.; writing—review & editing, Z.L., J.X., and G.T. All authors have read and agreed to the published version of the manuscript.

Funding: This research was funded by the Major Science and Technology Project of Xinjiang Uygur Autonomous Region, grant number 2018A03003, the Research on Mechanized Safety and Rapid Construction Technology of Extra-long Highway Tunnel, grant number 2018A03003-2, and the Fundamental Research Funds for the Central Universities of Central South University, grant number 2019zzts676.

Acknowledgments: The authors sincerely thank the support of the above fund project and the help of leaders and operators of the test site. Without these supports, the data and field test required by this research will not be able to completed.

Conflicts of Interest: The authors declare no conflict of interest.

References

1. Hu, Y.G.; Lu, W.B.; Chen, M.; Yan, P.; Yang, J.H. Comparison of Blast-Induced Damage Between Presplit and Smooth Blasting of High Rock Slope. *Rock Mech. Rock Eng.* **2013**, *47*, 1307–1320. [CrossRef]
2. Zhou, Z.; Cheng, R.; Cai, X.; Jia, J.; Wang, W. Comparison of Presplit and Smooth Blasting Methods for Excavation of Rock Wells. *Shock Vib.* **2019**, *2019*, 1–12. [CrossRef]
3. Zare, S.; Bruland, A. Comparison of tunnel blast design models. *Tunn. Undergr. Space Technol.* **2006**, *21*, 533–541. [CrossRef]
4. Jhanwar, J.; Jethwa, J. The use of air decks in production blasting in an open pit coal mine. *Geotech. Geol. Eng.* **2000**, *18*, 269–287. [CrossRef]
5. Kabwe, E. Improving Collar Zone Fragmentation by Top Air-Deck Blasting Technique. *Geotech. Geol. Eng.* **2016**, *35*, 157–167. [CrossRef]
6. Park, D.; Jeon, S. Reduction of blast-induced vibration in the direction of tunneling using an air-deck at the bottom of a blasthole. *Int. J. Rock Mech. Min. Sci.* **2010**, *47*, 752–761. [CrossRef]
7. Liu, K.Y.; Liu, B.G. Optimization of smooth blasting parameters for mountain tunnel construction with specified control indices based on a GA and ISVR coupling algorithm. *Tunn. Undergr. Space Technol.* **2017**, *70*, 363–374. [CrossRef]
8. Mandal, S.K.; Singh, M.M.; Dasgupta, S. Theoretical Concept to Understand Plan and Design Smooth Blasting Pattern. *Geotech. Geol. Eng.* **2008**, *26*, 399–416. [CrossRef]
9. Wang, J.; Yin, Y.; Luo, C. Johnson–Holmquist-II(JH-2) Constitutive Model for Rock Materials: Parameter Determination and Application in Tunnel Smooth Blasting. *Appli. Sci.* **2018**, *8*, 1675. [CrossRef]
10. Sumiya, F.; Kato, Y. A study on smooth blasting technique using detonating cords. *Sci. Technol. Energ. Mater.* **2007**, *68*, 167–170.
11. Dong, L.; Sun, D.; Shu, W.; Li, X. Exploration: Safe and clean mining on Earth and asteroids. *J. Clean Prod.* **2020**, *257*, 1–11. [CrossRef]
12. Lv, Y.; Jiang, Y.; Hu, W.; Cao, M.; Mao, Y. A review of the effects of tunnel excavation on the hydrology, ecology, and environment in karst areas: Current status, challenges, and perspectives. *J. Hydrol.* **2020**, *586*, 124891. [CrossRef]
13. Ding, L.; Zhang, L.; Wu, X.; Skibniewski, M.J.; Qunzhou, Y. Safety management in tunnel construction: Case study of Wuhan metro construction in China. *Saf. Sci.* **2014**, *62*, 8–15. [CrossRef]
14. Ko, Y.H.; Kim, S.J.; Yang, H.S. Assessment for the sympathetic detonation characteristics of underwater shaped charge. *Geosyst. Eng.* **2017**, *20*, 286–293. [CrossRef]
15. Victor, A.C. A simple method for calculating sympathetic detonation of cylindrical, cased explosive charges. *Propellants Explos. Pyrotech.* **1996**, *21*, 90–99. [CrossRef]
16. Kubota, S.; Liu, Z.Y.; Otsuki, M.; Nakayama, Y.; Ogata, Y.; Yoshida, M. A Numerical Study of Sympathetic Detonation in Gap Test. *Mater. Sci. Forum* **2004**, *465–466*, 163–168. [CrossRef]
17. DeFisher, S.; Baker, E.L.; Wells, L.; Quigley, G.; Lew, A. XM982 excalibur sympathetic detonation modeling and experimentation. In Proceedings of the Insensitive Munitions and Energetic Materials Technology Symposium, Bristol, UK, 24–28 April 2006; pp. 937–951.
18. Chen, L.; Wang, C.; Feng, C.G.; Lu, F.; Lu, J.Y.; Wang, X.F.; Guo, X. Study on Random Initiation Phenomenon for Sympathetic Detonation of Explosive. *Def. Technol.* **2013**, *9*, 224–228. [CrossRef]
19. Ishikawa, K.; Abe, T.; Kubota, S.; Wakabayashi, K.; Matsumura, T.; Nakayama, Y.; Yoshida, M. Study on the shock sensitivity of an emulsion explosive by the sand gap test. *Sci. Technol. Energy Mater.* **2006**, *67*, 199–204.
20. Chen, Q.K.; Xia, Y.W.; Liu, Z.F.; Wang, A.F.; Li, C.Y.; Yan, B.X. The Effect of Constraint Conditions on the Gap Distance of Emulsion Explosive. *Min. Res. Dev.* **2017**, *37*, 45–49. (In Chinese)

21. Katsabanis, P. Experimental and theoretical studies of sympathetic detonations in blastholes. In Proceedings of the 8th Annual Symposium on Explosives and Blasting Research, Orlando, FL, USA, 22–23 January 1992; pp. 17–26.
22. Zhang, F.H. The establishment of the empirical formula for calculating the gap distance in the blasthole. *Tunn. Constr.* **2003**, *23*, 7–9. (In Chinese)
23. Sućeska, M. *Test Methods for Explosives*; Springer: New York, NY, USA, 1995; pp. 45–47.
24. Yang, G.; Yang, R.; Jiang, L. Pressure distribution along borehole with axial air-deck charge blasting. *Explos. Shock Waves* **2012**, *32*, 653–657. (In Chinese)
25. Jhanwar, J.C.; Cakraborty, A.K.; Anireddy, H.R.; Jethwa, J.L. Application of Air Decks in Production Blasting to Improve Fragmentation and Economics of an Open Pit Mine. *Geotech. Geol. Eng.* **1999**, *17*, 37–57. [CrossRef]
26. Marchenko, L.N. Raising the efficiency of a blast in rock crushing. *Sov. Min.* **1982**, *18*, 395–399. [CrossRef]
27. Melnikov, N.V.; Marchenko, L.N. Effective Methods of Application of Explosion Energy in Mining and Construction. In Proceedings of the 12th U.S. Symposium on Rock Mechanics (USRMS), Rolla, MI, USA, 16–18 November 1970; pp. 359–378.
28. Lu, W.; Hustrulid, W. A Further Study on the Mechanism of Airdecking. *Fragblast* **2003**, *7*, 231–255. [CrossRef]
29. Sazid, M.; Singh, T.N. Mechanism of air deck technique in rock blasting-a brief review. In Proceedings of the 4th Indian Rock Conference, Mumbai, India, 29–31 May 2013; pp. 1–8.
30. Fourney, W.L.; Barker, D.B.; Holloway, D.C. Model studies of explosive well stimulation techniques. *Int. J. Rock Mech. Min. Sci. Geomech. Abstr.* **1981**, *18*, 113–127. [CrossRef]
31. Uotinen, L.; Janiszewski, M.; Baghbanan, A.; Caballero Hernandez, E.; Oraskari, J.; Munakka, H.; Szydlowska, M.; Rinne, M. Photogrammetry for recording rock surface geometry and fracture characterization. In Proceedings of the 14th International Congress on Rock Mechanics and Rock Engineering (ISRM 2019), Foz do Iguassu, Brazil, 13–18 September 2019; pp. 13–18.